PHYSICAL REVIEW A VOLUME 36, NUMBER 3 AUGUST 1, 1987

High-intensity multiphoton free-free transitions

R. Daniele, F. Trombetta, and G. Ferrante
Istituto di Fisica, via Archirafi 36, 90123 Palermo, Italy

P. Cavaliere and F. Morales
Dipartimento di Energetica e Applicazioni di Fisica, Parco d'Orleans, 90128 Palermo, Italy
(Received 17 November 1986; revised manuscript received 20 March 1987)

Based on a fundamental and simple treatment, selected calculations are performed of differential and total cross sections of multiphoton free-free transitions. The emphasis is on high values of the radiation field intensity such that the amplitude v_0 of the classical electron oscillatory velocity is equal or larger than the incoming velocity v_i. A variety of new information is obtained which gives a useful insight into various aspects of both the current theory and the physics of multiphoton free-free transitions. The calculations concern the following: (i) total cross sections in parallel and perpendicular geometry for both multiphoton emissions and absorptions, (ii) the breakdown of a known sum rule, (iii) the comparison of exactly calculated total cross sections with those based on widely used simplifications, and (iv) the investigation of the role of the range of scattering potential. Under particular conditions, the classical aspects of the elementary process (the interaction with the field) are found to affect the collision event and its characteristic parameters in a very peculiar way. The most interesting and new results are obtained when $v_0 \geqq v_i$ and $\mathbf{v}_0 \| \mathbf{v}_i$.

I. INTRODUCTION

This paper addresses the high-intensity aspects of multiphoton free-free transitions (MFFT), i.e., of the process in which, during the scattering of a charged particle by a structureless potential, an arbitrary number of photons is exchanged with a strong assisting laser field. Since the pioneering papers by Bunkin and Fedorov[1] and Kroll and Watson,[2] a lot of work has been devoted to MFFT. While many theoretical treatments of the MFFT have been worked out, the few available experiments so far have been necessarily concerned with only limited aspects of the process.[3–5] Detailed and updated accounts of the subject may be found now in several places, so we confine ourselves to quote some of them for the interested reader.[6–9]

As stated, this paper is concerned with the high-intensity limit of MFFT. There are several reasons for addressing this problem.

(1) In spite of the several theoretical papers available in the literature on the subject, the high-intensity behavior of the relevant parameters of the process (cross sections, mean-exchanged energy, etc.) is poorly understood. Most of the available practical information is given by estimates based on the asymptotic behavior of some special functions appearing in the theory. As it will be shown below, such estimates are of rather low reliability and have missed the new information which will be reported here. On the other hand, the first calculations considering the high-intensity domain have just sampled (and stopped at) the onset of an unexpected behavior of the MFFT cross sections. Doubts on the use of Volkov waves[10] and/or computational limitations[11] are likely to have been responsible for such incomplete investigation of this relevant aspect.

(2) Very intense lasers are now becoming available in pure research laboratories (up to 10^{16} W/cm^2), making real the possibility of investigating high-field effects also in MFFT.

(3) Finally, MFFT is one of the fundamental processes in laser plasma interactions, and efforts aimed at establishing a more accurate knowledge of the behavior of important parameters, required in applications, are expected to be useful.

In particular, we consider the scattering of electrons in the presence of a laser, taken as a single-mode homogeneous field, in the dipole approximation (model of an ideal laser). Of this process we calculate differential and total cross sections versus different quantities, including the field intensity. Concerning the scattering potential, the choice of a screened Coulomb potential offers in a simple way the possibility to get information on the role of the range of the potential when a strong radiation field interferes with the collision. Actual calculations are performed in first Born approximation, this being at the moment the only viable approximation allowing one to carry out a comprehensive set of calculations on different aspects of the process with a moderate use of computer time.

As far as the use of the ideal laser model is concerned, it is perhaps appropriate to mention that the present-day very intense lasers are likely to be poorly described by this model. Nevertheless, the understanding of MFFT in a strong laser field within the model of an ideal laser remains of obvious interest not only in its own right, but also as a necessary starting point for further improved and refined descriptions. The dipole approximation is adopted, so this amounts to saying that the typical velocities of the process must be smaller than the velocity of light. Accordingly, a nonrelativistic quantum treatment fits our

needs. The choice of the field parameters is such to obey the constraints of the dipole approximation. The present calculations, however, clearly call for a fully relativistic treatment, as a next step.

Most of the calculations are for a geometry in which the (linear) laser polarization is parallel to the beam of the incoming particles. An important role is found to be played in such geometry by the ratio v_0/v_i, with v_0 the amplitude of the classical oscillatory velocity of an electron in a plane-wave field, and v_i the initial particle velocity. Ratios v_0/v_i equal or larger than unity identify the high-intensity domain and are characteristic of the new results reported here. Unless stated otherwise, atomic units will be used.

II. DIFFERENTIAL AND TOTAL CROSS SECTIONS

The differential cross section (DCS) of the transition from the initial momentum $\mathbf{k}_i$ to $\mathbf{k}_f$, for an electron scattered by a static potential $V(r)$ in the presence of a strong ideal laser is given by the now familiar result[1,2]

$$\left[\frac{d\sigma}{d\Omega}\right]=\sum_n [k_f(n)/k_i]J_n^2(\lambda(n))\left[\frac{d\sigma(n)}{d\Omega}\right]=\sum_n\left[\frac{d\sigma}{d\Omega}\right]_n , \tag{2.1}$$

where

$$k_f(n)=k_i(1+2n\omega/k_i^2)^{1/2} \tag{2.2}$$

is the scattered electron momentum, with exchange of n photons ($n>0$ absorbed, $n<0$ emitted). $J_n(\lambda)$ is the Bessel function of the first kind, whose argument

$$\lambda(n)=\mathbf{E}_0\cdot\mathbf{Q}(n)/\omega^2,\quad \mathbf{Q}(n)=\mathbf{k}_f(n)-\mathbf{k}_i \tag{2.3}$$

represents the coupling strength between the field and the scattered particle; in it, $\mathbf{E}_0$ and ω are, respectively, the amplitude and the frequency of the field, assumed—as stated—to be homogeneous, single mode, purely coherent, linearly polarized, and taken in the dipole approximation as

$$\mathbf{E}(t)=\mathbf{E}_0\sin(\omega t) . \tag{2.4}$$

In (2.1), $d\sigma(n)/d\Omega$ has the structure of the field-free DCS. If the first Born approximation (FBA) for the scattering potential is used, it is calculated off the energy shell, at an incident energy $\varepsilon_i=k_i^2/2$ and final momentum $k_f(n)$ [Eq. (2.2)], and is given by

$$\left[\frac{d\sigma(n)}{d\Omega}\right]=(4\pi^2)^{-1}\left|\int d\mathbf{r}\exp[i\mathbf{Q}(n)\cdot\mathbf{r}]V(\mathbf{r})\right|^2 , \tag{2.5}$$

so that $d\sigma(0)/d\Omega$ is the FBA DCS for the field-free case. In the low-frequency limit $d\sigma(n)/d\Omega$ [in Eq. (2.1)] stands for the exact DCS or for any other suitable approximation going beyond the FBA, calculated on the energy shell at the shifted momenta[2]

$$\mathbf{q}_a(n)=\mathbf{k}_a-n\omega\mathbf{E}_0/[\mathbf{E}_0\cdot\mathbf{Q}(n)],\ a=i,f \tag{2.6}$$

provided a smooth energy dependence is exhibited by the pertinent T matrix and that $|\mathbf{E}_0\cdot\mathbf{Q}(n)|>n\omega^2$.

In this paper we shall choose the values of the parameters such as to allow us to use the FBA; accordingly $d\sigma(n)/d\Omega$ is given by (2.5). With the screened Coulomb potential

$$V(r)=(1/r)\exp(-r/r_0) , \tag{2.7a}$$

(2.5) gives

$$\frac{d\sigma(n)}{d\Omega}=\{2r_0^2/[1+r_0^2Q^2(n)]\}^2 . \tag{2.7b}$$

Large values of the range of the scattering potential ($r_0\gg1$) are expected to be only partially representative of the pure Coulomb case. In fact, the limit of infinitely long range in a screened Coulomb potential is a delicate problem in field-free collisions;[12] and by no means does it become easier when a strong radiation field is present.[13,14] Because of it, the pure Coulomb limit will not concern us here. We have a specific reason as well for this attitude here. As discussed in Ref. 12, one of the ways to correct the pathological (and unphysical) behavior of the pure Coulomb potential in theoretical treatments consists in introducing some cutoff in its range of action. It may be accomplished by means of an exponential screening, like in Eq. (2.7a), or just by an abrupt cutoff. The analysis shows[12] that provided sufficiently large screening radii are taken, the differently screened potentials yield results which are not distinguished by a typical Coulomb scattering experiment, in which forward scattering in a very narrow cone around the incoming direction is not observed. This conclusion implies also that in a very narrow cone of forward scattering there may be a large difference between the behavior and/or the results pertinent to the pure Coulomb potential and that of its screened versions. In the analysis given below, parts of the results are found to be peculiarly controlled by the behavior of the differential cross section at small scattering angles. Though the angular regions of interest here are considerably larger than those discussed in Ref. 12, the findings of the analysis of the Coulomb scattering suggest considering this part of our results as only partially representative of the Coulomb potential. Altogether, the results reported here are considered appropriate to a finite-range potential.

By (2.1), the total cross section (TCS) follows as

$$\sigma=\sum_n\sigma_n=\sum_n[k_f(n)/k_i]\int_{4\pi}d\Omega\,J_n^2(\lambda(n))\left[\frac{d\sigma(n)}{d\Omega}\right] . \tag{2.8}$$

Two classical parameters are found to play a key role in the problem under consideration. These are the amplitude of the classical oscillations an electron undergoes in the plane-wave field (2.4)

$$\alpha_0=E_0/\omega^2 \tag{2.9}$$

or, alternatively, the amplitude of the classical oscillatory velocity

$$v_0=E_0/\omega . \tag{2.10}$$

The basic particle-field coupling parameter (2.3) may be

expressed through α_0 or v_0 as

$$\lambda(n)=\boldsymbol{\alpha}_0\cdot\mathbf{Q}(n) \tag{2.3'}$$

and

$$\lambda(n)=\mathbf{v}_0\cdot\mathbf{Q}(n)/\omega\ . \tag{2.3''}$$

As it will be shown below, the most significant interplay between the (nonresonant) field and the collision process is found to occur when $\alpha_0 \geqq r_0$ and $v_0 \geqq v_i$, provided some other specific conditions are met. In other words, the field-dependent parameters α_0 and v_0 must be comparable with the characteristic parameters of the collision such as r_0 and v_i. In the FBA, it occurs generally for field intensities equal or larger than 10^{13} W/cm^2 for $\omega \simeq 1$ eV, which are well within the laboratory availability and the experimental state of the art. Below we shall concentrate mainly on just these domains.

We conclude this section by pointing out that the cross sections are derived within quantum-mechanical methods with, however, the laser field treated as an external classical field. The fact that the above classical parameters will be found to play an important role, together with the factored structure of the cross sections, suggests an interesting mixed picture of the laser-assisted scattering process. Namely, that of a process made up by two parts: the collisional part, which is described quantum mechanically, and the electron-laser interaction part, which result almost entirely classical. The requirement for the two parts to interfere and affect significantly each other is that their characteristic parameters be of comparable values. (It may be observed that the resonant interaction cases, not considered here, are no exception.)

III. CALCULATIONS: RESULTS AND COMMENTS

Below we report and comment on the results of our calculations. Unless specified otherwise, calculations are performed for an electron beam with an energy of 3.675 a.u. (100 eV) scattered by a Coulomb potential with a screening radius of 50 a.u. in the presence of a laser field, linearly polarized, parallel to the direction of the incoming particles. The energy of the laser photon is 0.043 a.u. (1.17 eV). The most frequently considered photon multiplicities are $n=1$, 5, and 10.

A. Enhancements and oscillations in the total cross sections. Parallel geometry ($\mathbf{E}_0 \| \mathbf{v}_i$)

Using the numerical values quoted above and the formula (2.8) we have calculated total cross sections in paral-

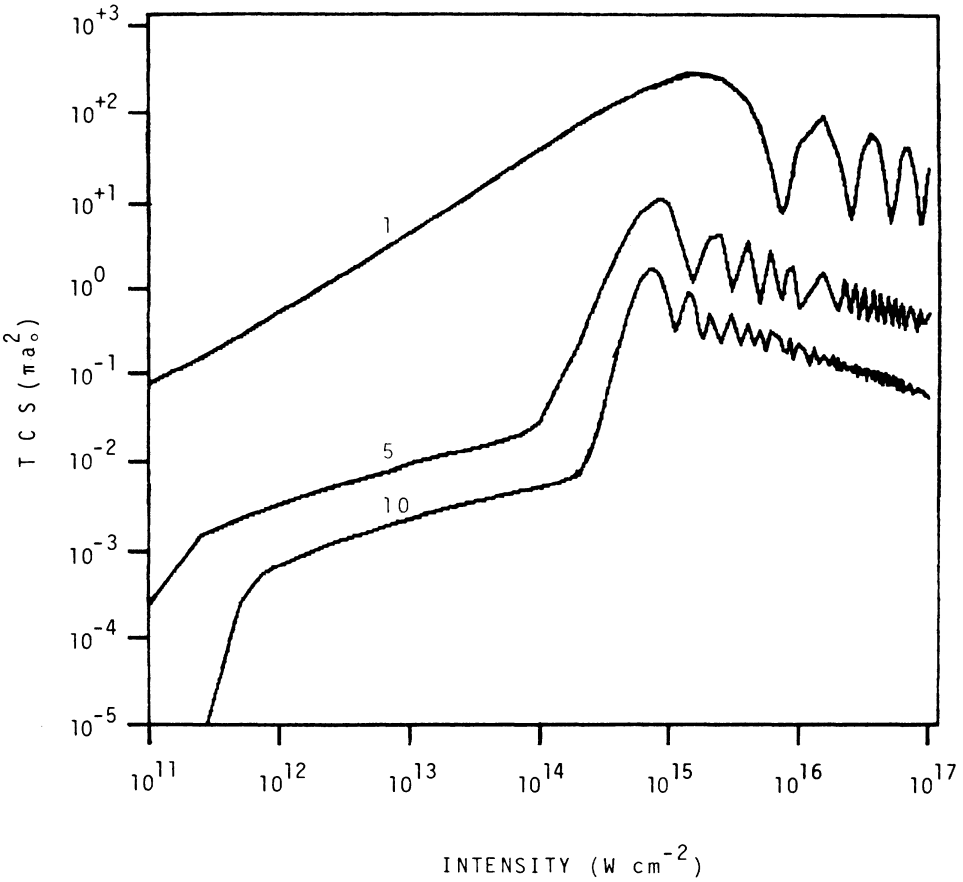

FIG. 1. Total cross sections (TCS) (in πa_0^2 units) vs the field intensity (in W/cm^2) for one, five, and ten photons absorbed. The incident particle energy is 100 eV, the field polarization is parallel to the incoming particle momentum, and the scattering potential is Yukawa type, with unitary charge and screening radius $r_0=50a_0$ (a_0 is the Bohr radius). Energy of the field photon $\hbar\omega=1.17$ eV.

lel geometry for the channels when during the scattering one, five, and ten field photons are absorbed. The results are presented in Fig. 1 as functions of the field intensity. The maximum value of the intensity is checked to be within the limits of validity of our theoretical model (nonrelativistic treatment, dipole approximation). Of course, by decreasing the laser frequency one could accordingly decrease the field intensity, without changing the general behavior.

The behavior of the reported TCS may be clearly divided into three different parts. (i) A perturbative I^n behavior is shown at (relatively) low intensities, (ii) at intermediate intensities, the TCS increase in a much slower way, thus showing a kind of saturation (with the exception of $n=1$, and $n=0$ not reported here), and (iii) for higher intensities, approximately at values when v_0 approaches v_i, the TCS show again a fast increasing behavior up to a maximum, after which a rather regular (in the average, decreasing) oscillatory behavior establishes. It is remarkable that the perturbative behavior for $n=1$ is found to hold up to very high values of the intensity and that the corresponding TCS is largely the dominant one among $n\neq 0$. As discussed by us elsewhere,[11] it is largely due to the strong averaging effect of the integration over the solid angle required to arrive at the total cross section.

A useful support to the numerical results of Fig. 1 may be obtained with the help of some simplifications of the exact formulas, yielding approximate analytical expressions of the high intensity TCS in parallel geometry. To this end, as an instance, we report in Figs. 2 and 3 the differential cross section for $n=1$ at two values of the intensity. Figure 2 is at 1.5×10^{15} W/cm^2, the intensity at which the TCS for $n=1$ reaches the first maximum. Figure 3 is at 8×10^{15} W/cm^2 and corresponds to the first minimum of the same TCS. The plotted DCS are also for different values of the potential screening parameter (which will be of interest below). Apart from the wild oscillatory behavior, similar to that known from different treatments,[15] at $r_0=50$ a.u. (at which the TCS of Fig. 1 are calculated) the DCS show a remarkable feature, which is profitably used below. Namely, the DCS are highly peaked in forward directions.

In order to perform a "peaking approximation" to be used to arrive at a simple analytical expression of the TCS, we observe that in the parallel geometry the particle field coupling $\lambda(n)$ may be expanded as

$$\lambda(n)=\lambda_1\sin^2(\theta/2)+n(\lambda_2+\lambda_3+\cdots)\cos\theta\ , \tag{3.1}$$

where θ is the scattering angle and

$$\lambda_1=-4(v_0/v_i)(\varepsilon_i/\omega)\ , \tag{3.2}$$

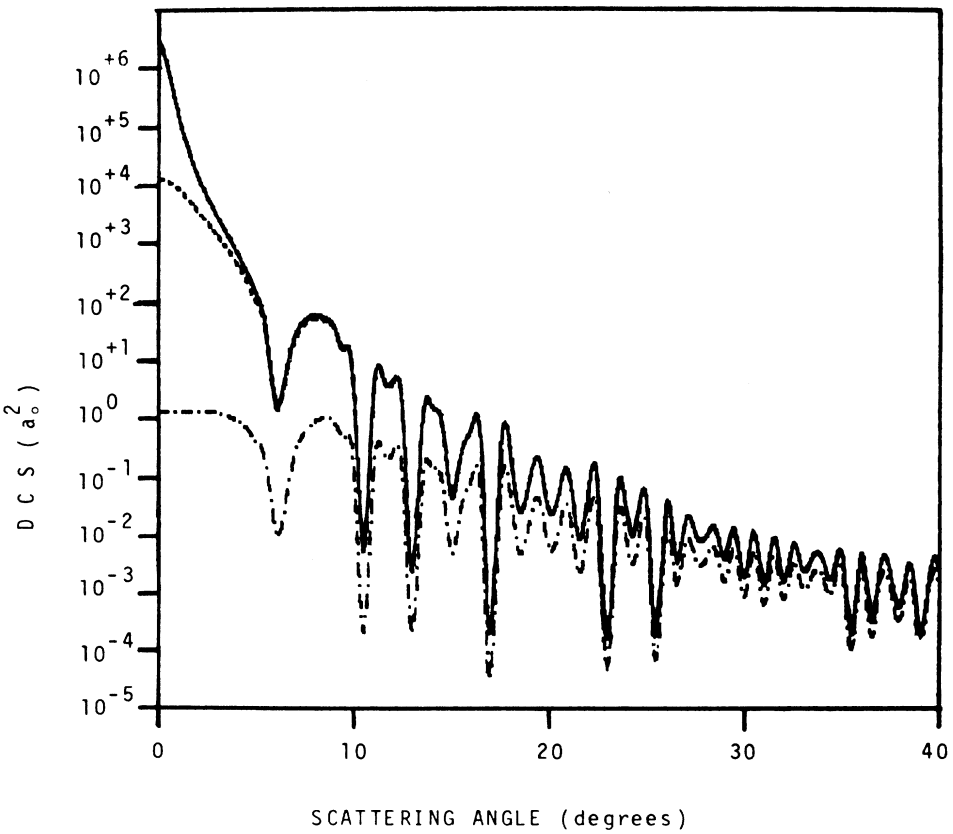

FIG. 2. Differential cross sections (DCS) (in $a_0^2\,\mathrm{sr}^{-1}$ units) vs the scattering angle (in degrees) for one photon absorbed, at a field intensity of $I=1.2\times 10^{15}$ W/cm^2 and various potential ranges $r_0=50a_0$ (solid line), $r_0=10a_0$ (dashed line), and $r_0=1a_0$ (dot-dashed line). Other parameters as in Fig. 1.

$$\lambda_2 = v_0/v_i \ , \tag{3.3}$$

$$\lambda_3 = -(1/4)(v_0/v_i)(n\omega/\varepsilon_i) \ . \tag{3.4}$$

According to (3.1)–(3.4) for $n\omega \ll \varepsilon_i$ and small scattering angles, the DCS corresponding to the exchange of n photons can be approximated as

$$\left[\frac{d\sigma}{d\Omega}\right]_n \simeq \frac{d\sigma(n)}{d\Omega} J_n^2[v_0(n-\theta^2\varepsilon_i/\omega)/v_i] \ . \tag{3.5}$$

When $\theta^2 \ll n\omega/\varepsilon_i$, a suitable approximation to the DCS is instead

$$\left[\frac{d\sigma}{d\Omega}\right]_n \simeq \frac{d\sigma(n)}{d\Omega} J_n^2(nv_0/v_i) \ . \tag{3.5a}$$

Next, expanding the squared momentum transfer in the small quantity $n\omega/k_i^2$,

$$Q^2(n) \simeq 2k_i^2\{2(1+n\omega/k_i^2)\sin^2(\theta/2) + [(n\omega/k_i^2)\cos\theta]/2\} \ ,$$

we note, first, that for $n \neq 0$ it does not vanish in the forward scattering, and, second, that for moderately long ranges (say, $r_0 \leqq 50$ a.u.), $d\sigma(n)/d\Omega$ may be taken as a function weakly dependent on n. Accordingly, rewriting (3.5a) as

$$\left[\frac{d\sigma}{d\Omega}\right]_n \simeq \frac{d\sigma(0)}{d\Omega} J_n^2(nv_0/v_i) \tag{3.5b}$$

for energetic electrons and/or moderately long-range potentials, the TCS may be approximately taken as

$$\sigma_n \simeq \sigma(0) J_n^2(nv_0/v_i) \ . \tag{3.6}$$

Needless to say that (3.5) and (3.6) are only demanded to reproduce some limiting qualitative behavior of the cross sections. Nevertheless, the agreement between exact numerical calculations and analytical predictions is satisfactory and provides further insight into the results. In fact, Eq. (3.6) accounts for the following: (i) for the enhancement occurring in TCS, Fig. 1, around $v_0 \simeq v_i$ (it is well known that $J_n(x)$ has its maximum at $n \simeq x$), (ii) for the harmoniclike oscillations and their n-proportional frequency, Fig. 1, and (iii) for the insensitivity on r_0 of the positions of the maxima and minima. This last feature may be seen by the large argument expansion of the Bessel function

$$J_n^2(nv_0/v_i) \simeq 2[\cos^2(nv_0/v_i - n\pi/2 - \pi/4)]/[(v_0/v_i)\pi n] \ . \tag{3.7}$$

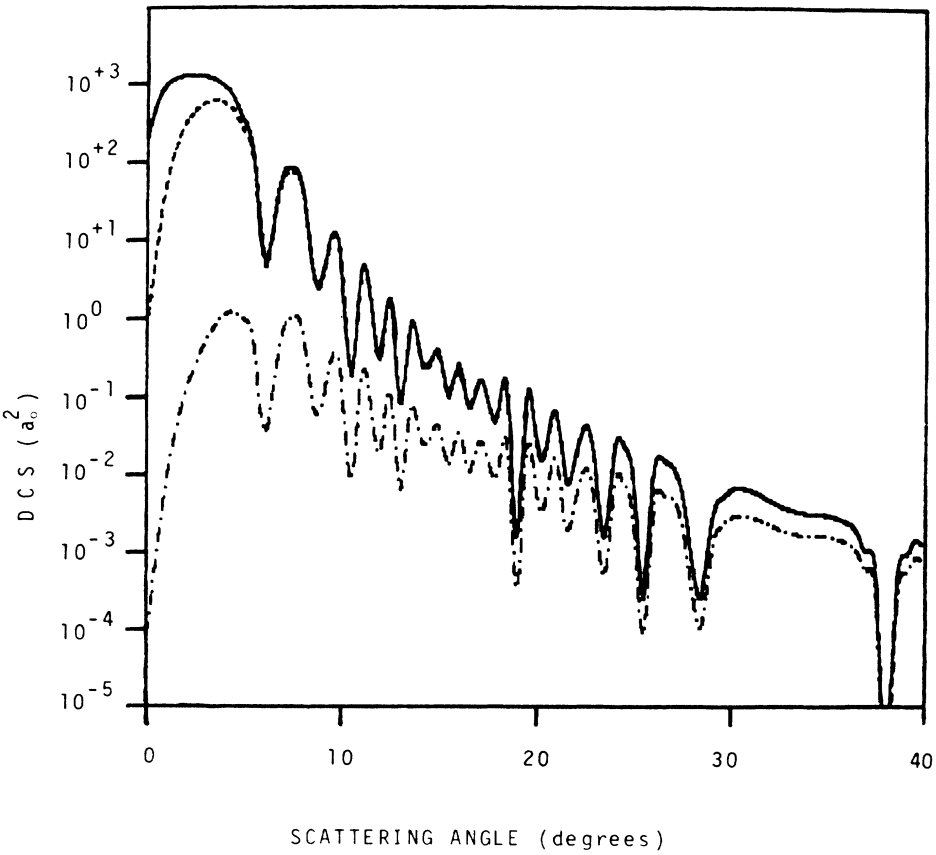

FIG. 3. Differential cross sections (DCS) (in $a_0^2\,\mathrm{sr}^{-1}$ units) vs the scattering angle (in degrees) for one photon absorbed at field intensity of $I = 8\times10^{15}$ W/cm^2. Other parameters as in Fig. 2.

We note that the finding that the behavior of the TCS under some circumstances is very sensitive to the condition

$$\lambda(n=0)=\lambda_1 \sin^2(\theta/2) \ll \lambda_2 \cos\theta$$

is likely to restrict to weak fields the validity of the approximate treatment for deriving the average number $\bar{n}$ of exchanged photons in MFFT, in which use is made of the expansion of $J_n^2(\lambda(n))$ in powers of $n\omega$ around $\lambda(0)$.[16] On the contrary, it well explains the resonantlike enhancement of $\bar{n}$ in the region $v_0 \simeq v_i$ as found in Ref. 17. Further, the limitation

$$|\mathbf{E}_0 \cdot \mathbf{Q}| > n\omega^2$$

necessary for deriving the Kroll and Watson result [Eq. (2.2) to all orders in the scattering potential with the shifted momenta (2.6)] makes the latter not suited for long-range potentials, energetic collisions, and TCS in the parallel geometry.

B. Total cross sections versus intensity and the range of the scattering potential

Figures 4 and 5 report calculations of the TCS for absorption of $n=1$ (Fig. 4) and $n=5$ (Fig. 5) photons versus the field intensity and for different values of the screening radius of the scattering potential ($r_0=50$, 10, and 1 a.u.). The main features of the reported calculations are (i) decreasing the screening radius of $V(r)$ from 50 to 10 a.u. the cross sections decrease, but the overall behavior remains. The oscillations too are maintained, though with reduced amplitude. (ii) Decreasing further r_0 up to 1 a.u., the TCS decrease further and any structure disappears. For several orders of magnitude of intensity, the TCS keep almost constant or slowly changing. Nothing particular happens at $v_0 \simeq v_i$; now the TCS are insensitive to v_0, which is thus found to play no role. Looking back at the DCS of Figs. 2 and 3 we see that for $r_0=1$ a.u. the small angle scattering has no particularly larger cross section as compared to those of scattering at large angles; accordingly for short-range potentials the peaking approximation is not allowed. The numerical calculations simply remind us that the physical situation with short-range potential is quite different as compared to that of relatively long-range ones. As a rich structure in the field-assisted TCS is found only for particular ranges of the potential and for intensity values such that $v_0 \geqq v_i$, we consider such a structure as the outcome of an interplay between the role of the scattering potential and the effect of strong-assisting radiation field.

C. Breakdown of a known sum rule

One of the most interesting and known results concerning the MFFT is the sum rule

$$\left[\frac{d\sigma}{d\Omega}\right] = \sum_n \left[\frac{d\sigma}{d\Omega}\right]_n \simeq \frac{d\sigma(0)}{d\Omega} \,. \tag{3.8}$$

Equation (3.8) implies that under particular conditions the differential cross sections in the presence of a laser field summed over all the multiphoton exchanges equal the field-free cross section for the same scattering process, taken at the same scattering angle and initial energy. The physical content of Eq. (3.8) is that the field does not change the number of particles scattered at a given angle, its effects being restricted to broadening and separating out the initially monochromatic energy distribution of

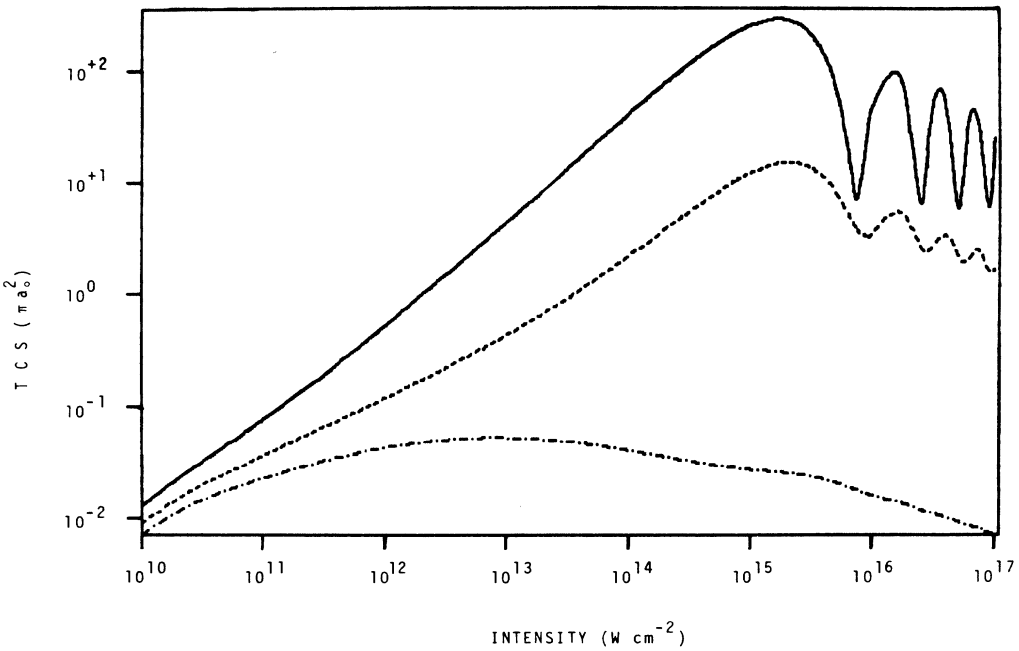

FIG. 4. Total cross sections (TCS) (in πa_0^2 units) vs the field intensity (in W/cm^2) for one photon absorbed and various potential ranges $r_0=50a_0$ (solid line), $r_0=10a_0$ (dashed line), and $r_0=1a_0$ (dot-dashed line). Other parameters as in Fig. 1.

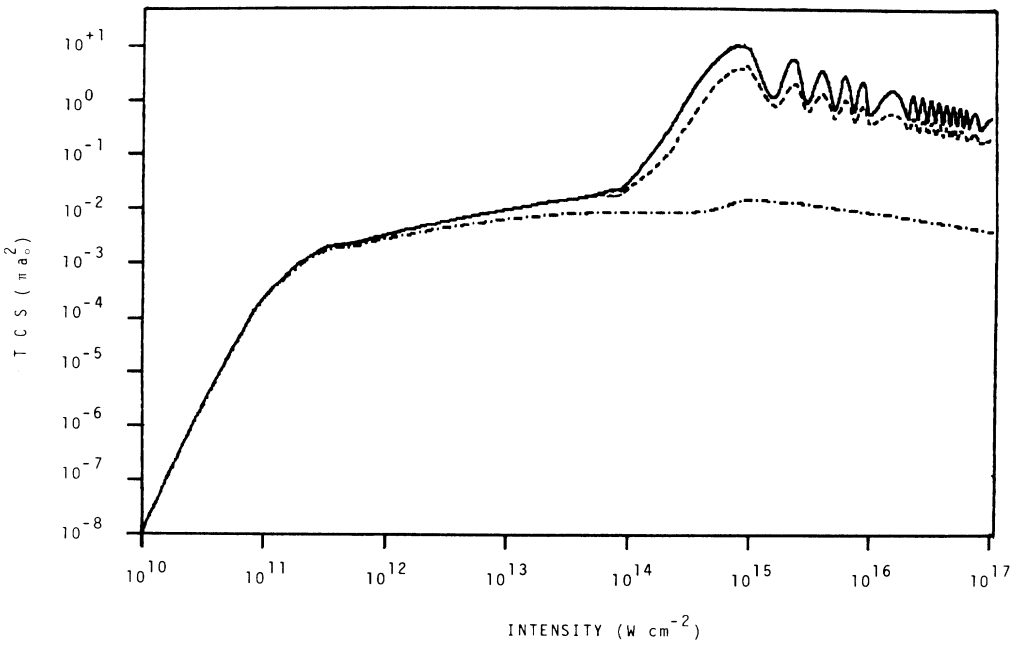

FIG. 5. Total cross sections (TCS) (in πa_0^2 units) vs the field intensity (in W/cm^2) for five photons absorbed. Other parameters as in Fig. 4.

scattered particles. Basically the conditions leading to (3.8) are believed to be the same as those which led us to obtain Eq. (3.5b), namely, $\varepsilon_i \gg n\omega$ and $d\sigma(n)/d\Omega$ an insensitive function of n. However, as we have just shown above and in more detail discussed elsewhere[18] it is true only when $v_0 \ll v_i$. Instead when $v_0 \simeq v_i$ a significant breakdown may occur in the sense that a cross section larger than the field-free one is obtained. To the discussion given previously, we wish to add a number of new considerations and results.

First, we note that for moderately long-range potentials, instead of (3.8), using (3.5), one has

$$\frac{d\sigma}{d\Omega} \simeq \frac{d\sigma(0)}{d\Omega}\left[J_0^2[\theta^2(v_0/v_i)(\varepsilon_i/\omega)] + \sum_n J_n^2(nv_0/v_i)\right], \tag{3.9}$$

for $\theta^2 < n\omega/\varepsilon_i$, $v_0 \simeq v_i$, parallel geometry, and small scattering angles. Equation (3.9) clearly shows that the field-assisted cross section is larger than the field-free one, the latter being provided practically by the $n=0$ term only. Equation (3.9) says also that for weak fields ($v_0 \ll v_i$), the expression in braces is approximately equal to unity.

For short-range potentials, Eq. (3.9) does not hold because the peaking approximation is not allowed. Nevertheless, the sum rule breaks down, though the departure from the field-free result is expected to be not very significant.

One may wonder about what happens for very-long-range potentials (hundreds of a.u.), when the peaking approximation is certainly valid. In this case too Eq. (3.9) does not hold, because now $d\sigma(n)/d\Omega$ is a sensitive function of n and cannot be taken out of the sum [see also the comments below Eq. (3.5a)]. Further, the sum rule is expected to be largely recovered because the $n=0$ channel will provide the by-large dominating contribution. Some typical results are shown in Fig. 6. Thus the conclusion is that, all the other conditions being the same, only po-

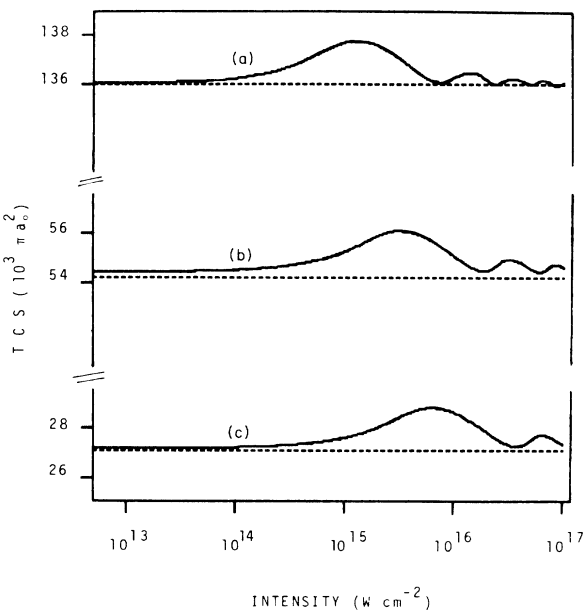

FIG. 6. Total cross sections (TCS) (in $10^3\pi a_0^2$ units) vs the field intensity (in W/cm^2), summed over all the multiphoton exchanges, for various incident particle energies (a) 100, (b) 250, and (c) 500 eV. The potential range is $r_0 = 500a_0$. Dashed lines, field-free TCS.

tentials of moderately long range lead to field-assisted cross sections larger than the field-free ones.

At the conditions at which Eq. (3.9) is valid, an approximate expression for the complete TCS is given by

$$\sigma=\sum_n \sigma_n \simeq \sigma_0 \left[1+\sum_{\substack{n \\ (n\neq 0)}} J_n^2(nv_0/v_i)\right] . \tag{3.10}$$

The sum over n entering Eq. (3.10) gives, for $v_0 < v_i$ (see the Appendix)

$$\sigma \simeq \sigma_0[1+(v_0^2/2v_i^2)F(\tfrac{3}{2},1;2;v_0^2/v_i^2)] , \tag{3.11}$$

where F is the hypergeometric function. Though meant to give only indications on the qualitative behavior of σ [$F(\frac{3}{2},1;2;x)$ diverges at $x\to 1$] Eq. (3.11) correctly shows the fast increasing of the summed TCS when v_0 approaches v_i.

D. Exact total cross sections versus estimates

For estimates of the cross sections in the high-intensity domain, the following asymptotic expression of the squared Bessel functions has been widely used:

$$J_n^2(x)\simeq 2[\cos^2(x-n\pi/2-\pi/4)]/\pi|x| , \tag{3.12}$$

with, as a rule, the additional simplification of approximating the fastly oscillating $\cos^2(\ )$ by its mean value $\frac{1}{2}$. Figures 7 and 8 compare TCS calculated exactly and using

$$J_n^2(x)\simeq 1/\pi|x| . \tag{3.12a}$$

This asymptotic expression is generally found to give large overestimates, besides, of course, missing the oscillatory structure. The departure from the exact results becomes even stronger for short-range potentials (Fig. 8), for which the exact TCS do not exhibit the complication of the oscillatory structure.

The agreement between estimates based on the proper asymptotic expressions of the Bessel functions and the exact calculation is apparently not improved if use is made of the method worked out in Ref. 19. To discuss briefly this point, we rewrite the integral of Eq. (2.8) in a different form (for parallel geometry)

$$\int_{4\pi} d\Omega\, J_n^2(\lambda(n))\frac{d\sigma(n)}{d\Omega}=4\pi\int_{1-\eta}^{1+\eta} dx\, F(x,\eta)J_n^2(\gamma x) , \tag{3.13}$$

with

$$\eta=k_f/k_i=(1+2n\omega/k_i^2)^{1/2} ,$$

$$\gamma=E_0k_i/\omega^2 ,$$

$$F(x,\eta)=d\sigma(n)/d\Omega .$$

According to Ref. 19, if the range of integration with respect to x in (3.13) includes the point $x=0$ (as our case does for absorption), a large factor containing $\ln\gamma \gg 1$ will additionally appear as compared with the result ob-

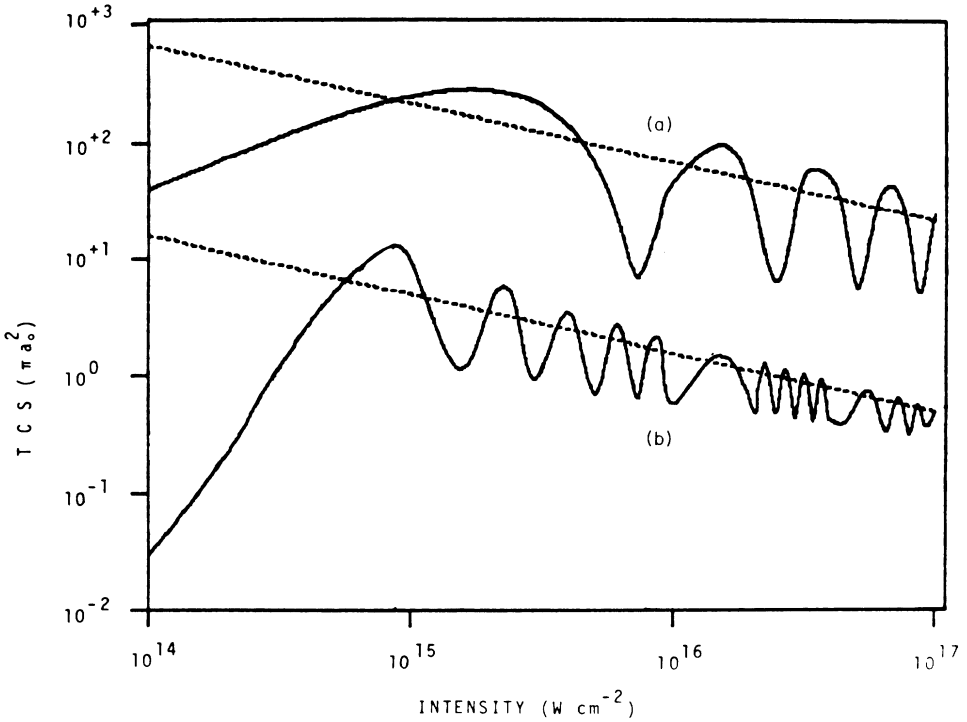

FIG. 7. Total cross sections (TCS) (in πa_0^2 units) vs the field intensity (in W/cm^2) calculated by the exact formula (2.1) (solid lines) and by using the large argument expansion of the Bessel function entering it (dashed lines), for (a) one and (b) five photons absorbed. Other parameters as in Fig. 1.

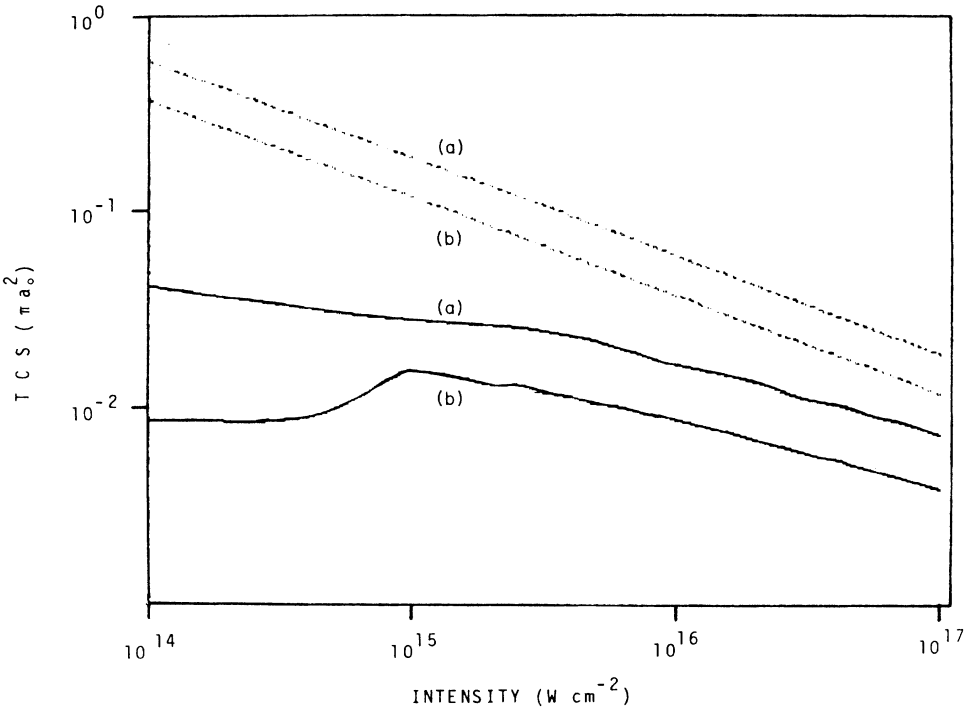

FIG. 8. Total cross sections (TCS) (in πa_0^2 units) vs the field intensity (in W/cm^2) calculated by the exact formula (2.1) (solid lines) and by using the large argument expansion of the Bessel function entering it (dotted lines), for (a) one and (b) five photons absorbed. The potential screening radius is $r_0 = 1a_0$. Other parameters as in Fig. 7.

tained when simply (3.12a) is used. Accordingly, an even larger overestimate will result.

E. Total cross sections. Perpendicular geometry ($\mathbf{E}_0 \perp \mathbf{v}_i$)

In Fig. 9 we report a set of calculations of the TCS versus the field intensity for the perpendicular geometry. Except for the field geometry, anything else is as in Fig. 1.

By comparison with Fig. 1, one sees that in the perpendicular geometry the enhancement about $v_0 \simeq v_i$ and the oscillations at $v_0 > v_i$ are completely absent. Instead, the general behavior of the TCS resembles that of TCS for short-range potentials (in parallel geometry), lowest curves

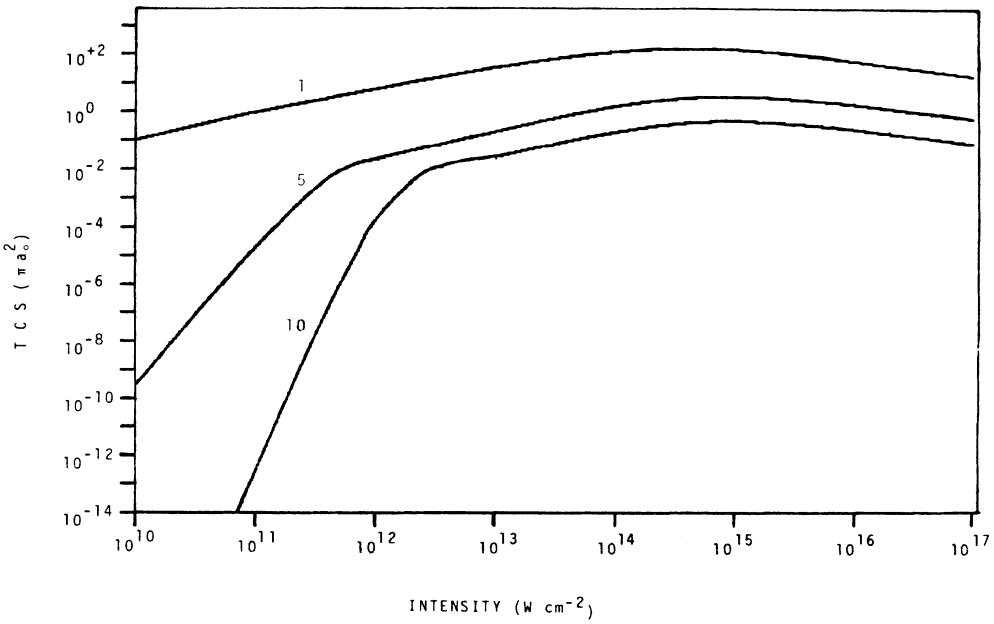

FIG. 9. Total cross sections (TCS) (in πa_0^2 units) vs the field intensity (in W/cm^2) for one, five and ten photons absorbed. The field polarization is perpendicular to the incoming particle momentum. Other parameters as in Fig. 1.

of Figs. 4 and 5. In perpendicular geometry all the terms of the expansion (3.1) have the same angular dependence, so that a result like (3.6) cannot be arrived at. On the other hand, the exact numerical evaluation of the TCS shows that nothing particular happens at $v_0 \simeq v_i$. Thus, as in the case of short-range potentials in parallel geometry, in the perpendicular geometry the classical parameter v_0 is found not to play a particularly significant role.

F. Total cross sections with photon absorption versus total cross sections with emission

Up to now all the reported calculations have been confined to collision events followed by photon absorptions. For completeness and further insight into the physics of the elementary process, in Figs. 10–12 we report TCS for photon emission as well and compare them with those for photon absorption (in parallel geometry). The comparison shows expected similarities but instructive differences as well. The cross sections for absorption and emission of one photon are largely the same both in absolute values and in shape. The differences between emissions and absorptions are better seen in the TCS of high multiplicity. The perturbative portions of the TCS with emission and absorption of high multiplicity as well are largely the same.

For multiphoton exchanges, starting from the onset of the nonperturbative behavior up to the first peak, emissions have larger TCS than absorptions. In this interval of intensities the shapes of the two TCS too are different. The TCS for emission shows steady increase, while that for absorption shows a kind of saturation.

The physical interpretation of these different behaviors is straightforward, and is based on the consideration that the electrons are simultaneously undergoing a translational motion at v_i and an oscillatory motion parallel to v_i, at a velocity of amplitude v_0. At intensities for which still $v_i > v_0$ photon emissions are favored because the lowering of the electron translational velocity favors the matching of v_i with v_0 and thus a "resonance" condition. At the same intensities, photon absorptions are saturated, because such processes, increasing the electron velocity v_i, only worsen the matching condition.

The same interpretation helps to understand the slightly reversed (though less marked) behavior occurring in the oscillatory parts of the TCS, past the first peak (Fig. 12). We observe that this situation is strongly reminiscent of a well-known classical process occurring in plasma physics, namely, that of two-stream instability, which is frequently viewed also as a kind of Čerenkov effect.

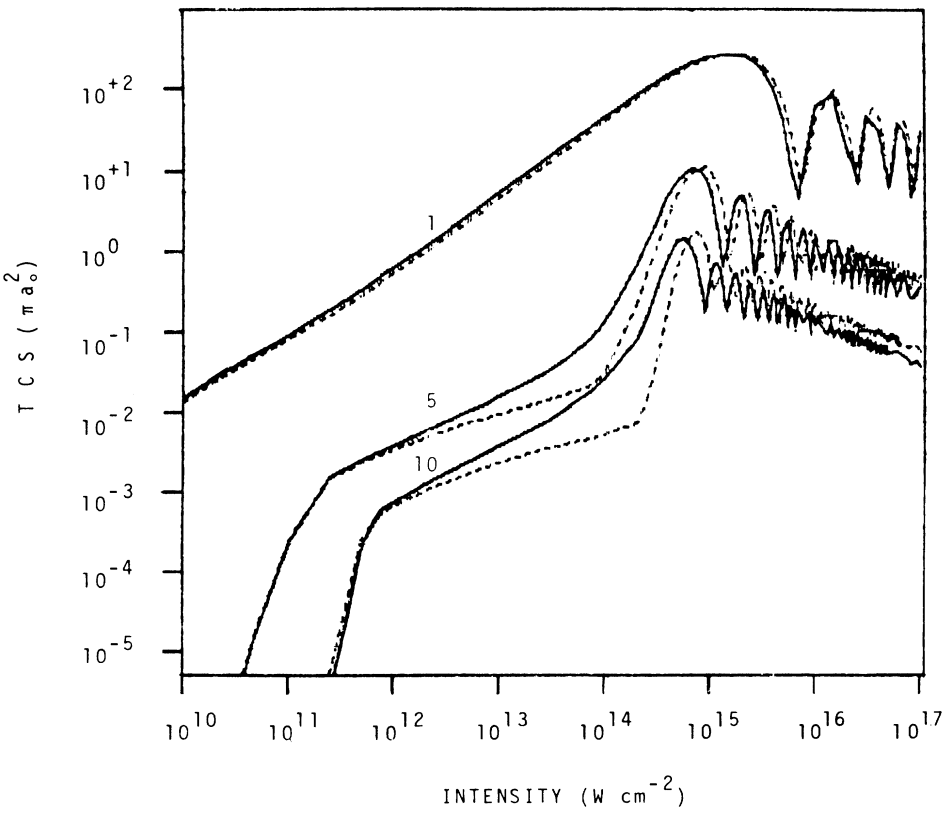

FIG. 10. Total cross sections (TCS) (in πa_0^2 units) vs the field intensity (in W/cm^2) for absorption (dashed lines) and emission (solid lines) of one, five and ten photons. Other parameters as in Fig. 1.

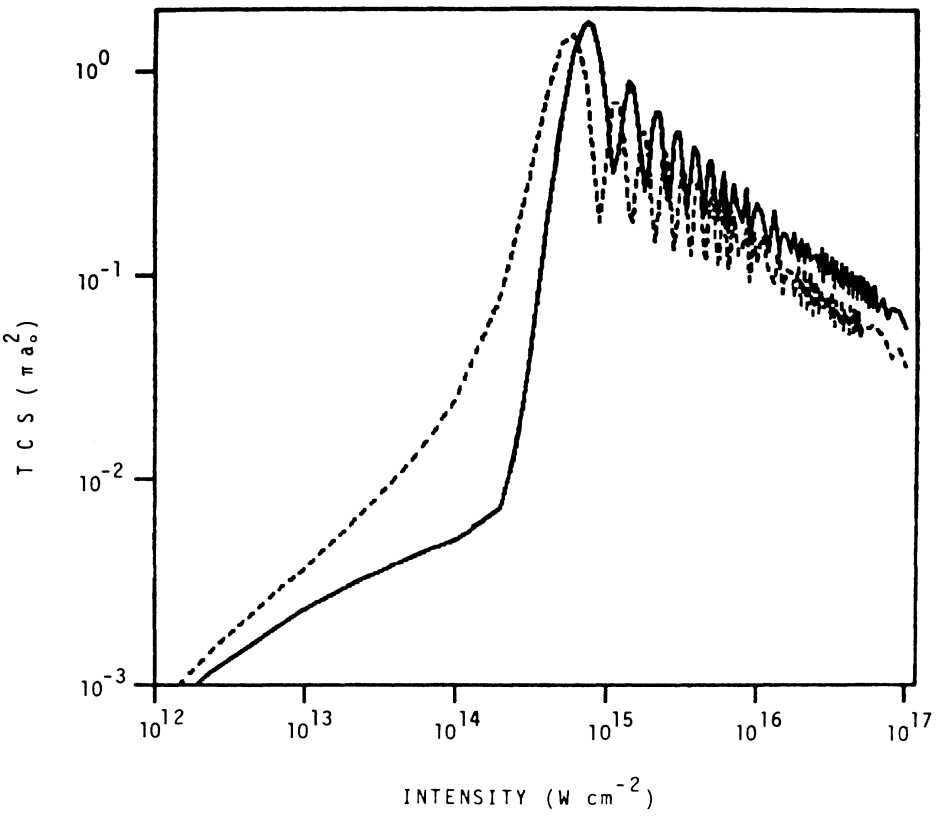

FIG. 11. Total cross sections (TCS) (in πa_0^2 units) vs the field intensity (in W/cm^2) for absorption (solid line) and emission (dashed line) of ten photons. Other parameters as in Fig. 1.

IV. AN APPROXIMATE EIKONAL TREATMENT OF FREE-FREE TRANSITIONS

All of the reported results are based on the first Born formulas exactly calculated. Besides, an effort has been made to single out from the FBA formulas the dominating features to be able to have a check of the numerical results. As we believe, altogether it has helped to have a fuller insight into the results exhibiting several interesting physical aspects.

We have considered relatively energetic collisions to be allowed to use the FBA. Nevertheless, we are aware of the limit of the Born approximation, especially from a quantitative point of view. Qualitatively, instead, the reported results should be confirmed also by more accurate theoretical treatments. In this sense, the merits of the FBA are in that it allows us to get a first comprehensive picture of many physical aspects in a relatively simple and unified way. Unfortunately, more rigorous treatments are much more difficult to handle and to date they may serve only for giving limited answers to single questions.

It is of interest to consider here the eikonal approximation to the problem at hand here.[20,21] We wish to show that performing reasonable simplifications and considering some special cases, from the exact eikonal cross section one may obtain expressions clearly reproducing the same physical contents as those discussed above.

We find it convenient to start with the general expression for the eikonal total cross section in the form derived by Gersten and Mittleman [formula (3.4) of Ref. 20]; namely, changing slightly the original notation

$$\sigma^E = 4\int d^2b \int_0^{2\pi} (2\pi)^{-1} da \sin^2 \times \left[\sum_{-\infty}^{+\infty} J_n(n v_0/v_i) \times \exp(-ina)\chi_n(b,v_i) \right] \quad (4.1)$$

with

$$\chi_n(b,v_i) = (2v_i)^{-1} \int_{-\infty}^{+\infty} V(b,z) \exp(-in\omega z/v_i) dz \quad (4.2)$$

quantities strictly related to the eikonal phase-shift functions. In fact, $n=0$ gives

$$\chi_0(b,v_i) = (2v_i)^{-1} \int_{-\infty}^{+\infty} V(b,z) dz \ , \quad (4.3)$$

the field-free eikonal phase-shift function, while χ_n with $n \neq 0$ multiplied by $[J_n(n v_0/v_i)\exp(-ina)]$ give the contributions due to the field. Accordingly, Eq. (4.1) is rewritten as

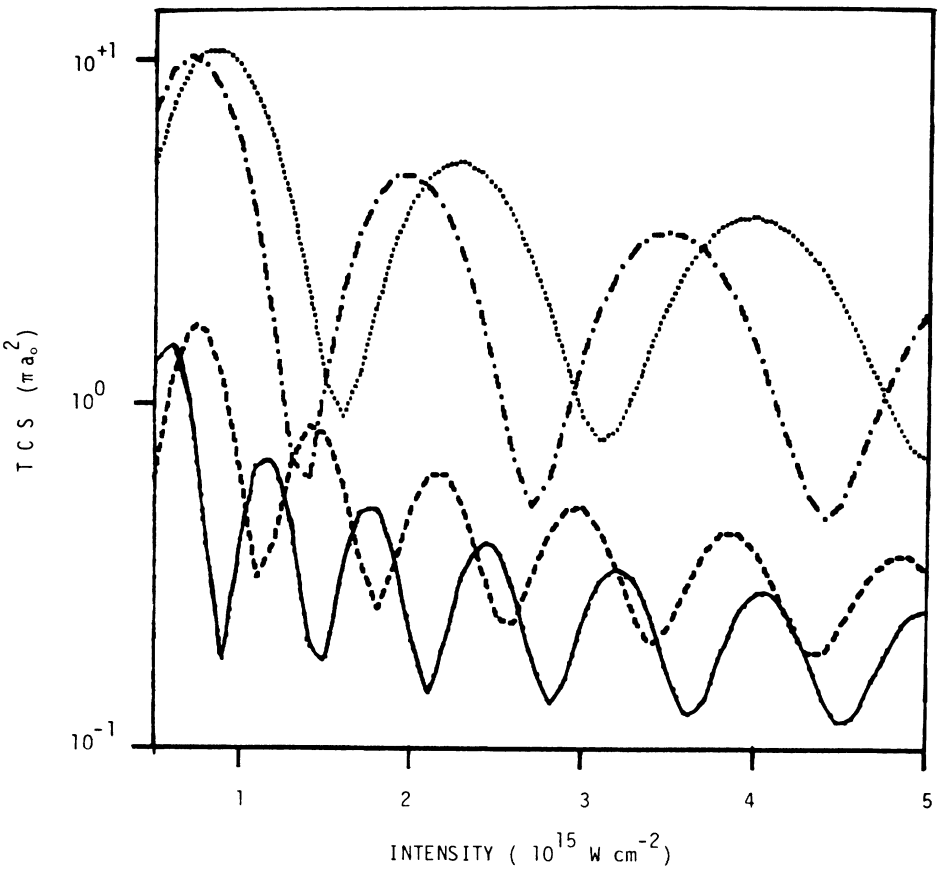

FIG. 12. Total cross sections (TCS) (in πa_0^2 units) vs the field intensity (in W/cm^2). Details of Fig. 10 concerning the oscillatory structure. Dotted line, absorption of five photons; dot-dashed line, emission of five photons; dashed line, absorption of ten photons;

$$\sigma^E=4\int d^2b\int_0^{2\pi}(2\pi)^{-1}da\,\sin^2 \times\left[\chi_0+\sum_{\substack{n\\(n\neq 0)}} J_n(nv_0/v_i)\times\exp(-ina)\chi_n(b,v_i)\right]. \tag{4.4}$$

Now, we assume that the scattering potential is such that χ_n is weakly dependent on n. Generally, even in strong-field contexts, only small n count, so that the assumption of weak n dependence for χ_n is reasonable for finite-range potentials and high energies [see below, Eq. (4.15)]. Thus we can take χ_n out of the infinite sum over n in (4.4) either letting $n=0$ or, alternatively, taking some average value of n, say $\bar{n}$,

$$\sum_{\substack{n\\(n\neq 0)}} J_n(nv_0/v_i)\exp(-ina)\chi_n(b,v_i) \simeq 2\chi_{\bar{n}}(b,v_i)\sum_{n=1}^{\infty}\cos(na)J_n(nv_0/v_i)\,. \tag{4.5}$$

With the constraint

$$\left|\frac{x}{1+(1-x^2)^{1/2}}\exp[(1-x^2)^{1/2}]\right|<1 \tag{4.6}$$

implying $x=v_0/v_i<1$, and using the result N.5.7.32.1 of Ref. 22, the sum over n in (4.5) is performed to give

$$\sum_{n=1}^{\infty}\cos(na)J_n(nv_0/v_i)=(v_0/2v_i)\cos\beta[1-(v_0/v_i)\cos\beta]^{-1}\,, \tag{4.7}$$

with β defined by the equation

$$\beta-(v_0/v_i)\sin\beta=a\,. \tag{4.8}$$

During the integration over a, when $\cos\beta\simeq 1$, Eq. (4.7) becomes very large if additionally $v_0\simeq v_i$. In such a case, the contributions to the eikonal phase-shift function due to the field are strongly enhanced, in agreement with our previous findings, and the total cross section is expected to be considerably modified.

We now make the assumption that the field-free eikonal phase-shift function χ_0 is much larger than the contributions due to the field, and expand, accordingly, the sine function of Eq (4.4). It gives

$$\sigma^E \simeq \sigma^E_{\rm FF} + 8v_i^2 \sum_{n=1}^{\infty} J_n^2(nv_0/v_i) \times \int d^2b \cos(2\chi_0) \, | \chi_n(b,v_i) |^2 , \quad (4.9)$$

with $\sigma_{\rm FF}$ the field-free cross section, and χ_0 and χ_n given, respectively, by (4.3) and (4.2). This result, which is very similar to Eq. (3.13) of Ref. 20, is rich in information concerning the behavior of the cross section and this information is in close qualitative agreement with the findings of our previous sections. With the constraint (4.6) and letting again $n \to \bar{n}$ in χ_n, the summation in (4.9) is performed with the aid of the relation N.5.7.31.1 of Ref. 22 (an alternative expression is derived in the Appendix), and we have the expression

$$\sigma^E \simeq \sigma^E_{\rm FF} + 4v_i^2 \, | \chi_{\bar{n}} | [(1 - v_0^2/v_i^2)^{1/2} - 1]^{-1/2} \int d^2b \cos(2\chi_0) \quad (v_0/v_i < 1) . \quad (4.10)$$

Finally, assuming sufficiently high initial velocities and weak potentials, we approximate the sine appearing in Eq. (4.1) by its argument and readily obtain formulas very similar to the FBA ones (as it should be). In fact, we have

$$\sigma_0^E \simeq (\sigma^E_{\rm FF})_0 + \sum_{\substack{n \\ (n \neq 0)}} J_n^2(nv_0/v_i) \sigma_0^E(n) , \quad (4.11)$$

$$(\sigma^E_{\rm FF})_0 = 4 \int d^2b \chi_0^2(b,v_i) \quad (4.12)$$

and

$$\sigma_0^E(n) = 4 \int d^2b \, | \chi_n(b,v_i) |^2 . \quad (4.13)$$

Further, if for the n values which count $\sigma_0^E(n)$ is a weak function of n, Eq. (4.11) may be rewritten as

$$\sigma_0^E \simeq (\sigma^E_{\rm FF})_0 \left[1 + \sum_{\substack{n \\ (n \neq 0)}} J_n^2(nv_0/v_i) \right] . \quad (4.14)$$

The approximate cross sections derived in this section have their origin in the eikonal treatment, but show largely the same behavior as their FBA counterparts (3.5), (3.6), (3.9), and (3.10); accordingly, they express largely the same physical contents (breakdown of the sum rule, favorable conditions for enhancement of the cross sections at $v_0 \simeq v_i$, oscillatory behavior at $v_0 > v_i$, and so on).

For the potential considered in our calculations,

$$V(r) = V(b,z) = r^{-1} \exp\{ -[(b^2 + z^2)^{1/2}]/r_0 \} ,$$

we have

$$\chi_n(b,v_i) = (v_i)^{-1} K_0(b(n^2\omega^2/v_i^2 + 1/r_0^2)^{1/2}) , \quad (4.15)$$

where $K_0(z)$ is the zero-order cylindrical function of an imaginary argument and use has been made of the integral (3.962.2) of Ref. 23. The argument of K_0 clearly shows when the n dependence may be neglected and which is the role of the range of the potential. With a choice of the parameters convenient to the approximation adopted, and considering that contributions with small n dominate in the total cross section, we may conclude that in (4.15) the n dependence is negligible. So, within an eikonal treatment of strong-field free-free transitions, we have ended, qualitatively, with the same conclusions arrived at in the first Born approximation. Quantitatively, the actual results may well be different. It is worth noting the fact that in the eikonal treatment some dominating features have emerged almost immediately, while in the case of the first Born approximation an inspection of the pertinent formulas has been required coupled to preliminary calculations of the DCS. It is due to the peculiar features of the eikonal approximation itself.

V. CONCLUDING REMARKS

In this work, based on a basic and simple treatment (first Born approximation and ideal laser model), we have performed a comprehensive set of numerical high-intensity calculations, which have produced a variety of new information, believed to prompt other, more accurate investigations.

In particular, we have found the following: (i) the behavior of the total cross section versus intensity may significantly depend on the range of the scattering potential, (ii) for moderately long-range potentials, in parallel geometry $\mathbf{k}_i // \mathbf{E}_0$, the total cross sections show an enhancement by orders of magnitude when $v_0 \simeq v_i$, and an oscillatory behavior when $v_0 > v_i$, and (iii) near $v_0 \simeq v_i$, scattering events with absorption have a cross section of different form as compared to that of scattering with emission. A physical explanation has been provided to this result.

Being based on the first Born approximation, the reported results are expected to be only qualitatively correct. However, as most of the results have a rather transparent physical interpretation, they are expected to hold in an essential way also beyond the FBA. Accordingly, it is hoped that comprehensive and more rigorous calculations will soon become available on the same subject.

A basic feature underlying most of the obtained results is the interplay between the classical and the quantum aspects of the elementary process. This interplay is formally expressed by the factored structure of the differential cross sections, Eq. (2.1). Several numerical results and some specific analytical expressions say that the classical aspects of the process manifest themselves only when the large majority of the particles interact efficiently with the field (parallel geometry and moderately long-range potentials). When it happens, the classical parameters entering the theoretical treatment are found to play a key role and the scattering parameters strongly affected. When instead only few electrons, for one reason or another (short-range potentials and/or perpendicular geometry), interact strongly with the field, no peaking approximation is allowed, the classical aspects of the process are smeared out by the integration over the angles and practically lost.

The emphasis of the calculations has been on the high-intensity domains. As stated in the Introduction, for such domains the ideal laser model is likely to be a rather poor representation of a real intense laser. Nevertheless, the reported information is believed to be significant because,

first, the ideal laser model is a fundamental model, on which the great majority of theoretical predictions is usually based; second, it serves as a necessary starting point for more refined and realistic treatments.

ACKNOWLEDGMENTS

The authors express their thanks to the University of Palermo Computational Centre for the computer time generously provided to them. This work was supported by the Italian Ministry of Education, the National Group of Structure of Matter, and the Sicilian Regional Committee for Nuclear and Structure of Matter Researches.

APPENDIX

In this appendix we evaluate the sum

$$S(x)=\sum_{n=1}^{\infty} J_n^2(nx) \ .$$

Using the integral representation of the squared Bessel function

$$J_n^2(nx)=(2/\pi)\int_0^{\pi/2} d\theta J_{2n}(2nx\cos\theta) \ , \tag{A1}$$

we have

$$S(x)=(2/\pi)\int_0^{\pi/2} d\theta f(\theta) \ , \tag{A2}$$

where

$$f(\theta)=\sum_{n=1}^{\infty} J_{2n}(2nx\cos\theta)$$

$$=(x^2\cos^2\theta)/[2(1-x^2\cos^2\theta)] \tag{A3}$$

provided that

$$x\cos\theta<[1+(1-x^2\cos^2\theta)]^{-1/2}\exp[-(1-x^2\cos^2)^{1/2}] \ , \tag{A4}$$

implying, as a limit, $x<1$.

Integration of $f(\theta)$ in (A2) gives

$$S(x)=(x^2/4)F(\tfrac{3}{2},1;2;x^2) \ , \tag{A5}$$

with F the hypergeometric function. (A5) is used in the main text [Eq. (3.11)]. An alternative expression may be found in Ref. 22, N.5.7.31.1, and is used in Eq. (4.10). All the formulas used in this appendix can be found in Ref. 23.

[1]F. V. Bunkin and M. V. Fedorov, Zh. Eksp. Teor. Fiz. **49**, 31 (1965) [Sov. Phys.—JETP **22**, 844 (1966)].

[2]N. M. Kroll and K. M. Watson, Phys. Rev. A **8**, 804 (1973).

[3]A. Weingartshofer, J. K. Holmes, J. Sabbagh, and S. L. Chin, J. Phys. B **16**, 1805 (1983).

[4]L. Langhans, J. Phys. B **11**, 2361 (1978).

[5]D. Andrick and H. Bader, J. Phys. B **17**, 4549 (1984).

[6]M. H. Mittleman, *Introduction to the Theory of Laser-Atom Interactions* (Plenum, New York, 1982).

[7]L. Rosenberg, Adv. At. Mol. Phys. **18**, 1 (1982).

[8]F. Ehlotzky, Can. J. Phys. **63**, 907 (1985).

[9]G. Ferrante, in *Fundamental Processes in Atomic Collisions Physics,* edited by H. Kleinpoppen, H. O. Lutz, and J. S. Briggs (Plenum, New York, 1985), p. 343.

[10]H. Brehme, Phys. Rev. C **3**, 837 (1971).

[11]R. Daniele, G. Ferrante, and R. Zangara, Nuovo Cimento D **2**, 1509 (1983).

[12]J. Taylor, *Scattering Theory* (Wiley, New York, 1972), Sec. 14-1.

[13]J. Banerji and M. H. Mittleman, Phys. Rev. A **26**, 3706 (1982).

[14]L. Rosenberg, Phys. Rev. A **20**, 457 (1979).

[15]R. Shakeshaft, Phys. Rev. A **28**, 667 (1983).

[16]M. H. Mittleman, Phys. Rev. A **21**, 79 (1980).

[17]S. Bivona, R. Zangara, and G. Ferrante, Phys. Lett. **110A**, 375 (1985).

[18]R. Daniele, G. Ferrante, F. Morales, and F. Trombetta, J. Phys. B **19**, L133 (1986).

[19]R. V. Karapetyan and M. V. Fedorov, Sov. J. Quantum Electron. **7**, 1260 (1977).

[20]J. I. Gersten and M. H. Mittleman, Phys. Rev. A **12**, 1840 (1975).

[21]G. Ferrante, C. Leone, and L. Lo Cascio, J. Phys. B **12**, 2319 (1979).

[22]A. P. Prudnikov, Yu. A. Brychkov, and O. I. Marichev, *Special Functions, Integrals and Series* (in Russian) (Nauka, Moscow, 1983).

[23]I. S. Gradshteyn and I. M. Ryzhik, *Tables of Integrals, Series, and Products* (Academic, New York, 1973).